GEOCHEMISTRY AND U-PB ZIRCON AGE OF THE INTERNAL OSSA-MORENA ZONE OPHIOLITE SEQUENCES: A REMNANT OF RHEIC OCEAN IN SW IBERIA

Jorge Pedro*,✉, Alexandre Araújo, Paulo Fonseca***, Colombo Tassinari°** and **António Ribeiro°°**

* *Departamento de Geociências, Universidade de Évora and Centro de Geologia, Universidade de Lisboa, Portugal.*
** *Departamento de Geociências and Centro de Geofísica, Universidade de Évora, Portugal.*
*** *Departamento de Geologia and Centro de Geologia, Universidade de Lisboa, Portugal.*
° *Centro de Pesquisas Geocronológicas, Instituto de Geociências, Universidade de São Paulo, Brasil.*
°° *Centro de Geologia, Universidade de Lisboa, Portugal.*
✉ *Corresponding author, e-mail: jpedro@uevora.pt*

Keywords: *Ophiolite, Rheic Ocean, Early Ordovician, SW Iberia, Ossa-Morena Zone. Portugal.*

ABSTRACT

The Early Paleozoic geodynamic evolution in SW Iberia is believed to have been dominated by the opening of the Rheic Ocean. The Rheic Ocean is generally accepted to have resulted from the drift of peri-Gondwanan terranes such as Avalonia from the northern margin of Gondwana during Late Cambrian-Early Ordovician times. The closure of the Rheic Ocean was the final result of a continent-continent collision between Gondwana and Laurussia that produced the Variscan orogen. The Ossa-Morena Zone is a peri-Gondwana terrane, which preserves spread fragments of ophiolites - the Internal Ossa-Morena Zones Ophiolite Sequences (IOMZOS). The final patchwork of the IOMZOS shows a complete oceanic lithospheric sequence with geochemical characteristics similar to the ocean-floor basalts, without any orogenic fingerprint and/or crustal contamination. The IOMZOS were obducted and imbricated with high pressure lithologies. Based on structural, petrological and whole-rock geochemical data, the authors argue that the IOMZOS represent fragments of the oceanic lithosphere from the Rheic Ocean. Zircon SHRIMP U-Pb geochronological data on metagabbros point to an age of ca. 480 Ma for IOMZOS, providing evidence of a well-developed ocean in SW Iberia during this period, reinforcing the interpretation of the Rheic Ocean as a wide ocean among the peri-Gondwanan terranes during Early Ordovician times.

INTRODUCTION AND GEOLOGICAL SETTING

The evolution of the SW European Variscides started in the Late Cambrian, when the Rheic Ocean opened along the northern margin of Gondwana as a result of the drift of Avalonia and Armorica/Iberia (peri-Gondwanan terranes). This evolution culminated in the Devonian-Carboniferous, characterized by the occurrence of subduction/obduction followed by continent-continent collision during the formation of Pangea (Ribeiro et al., 2007; 2010). The evolutionary steps could be identified by bimodal volcanism (preserving stages of rifting evolution), ophiolite terranes (in scattered outcrops), HP-rock assemblages (i.e., eclogites and blueschits) and continental allochthonous terranes. Additionally, remnants of the Rheic Ocean, the Internal Ossa-Morena Zone Ophiolite Sequences (IOMZOS), can be found in the SW Iberia Variscides. IOMZOS are interpreted as oceanic lithosphere fragments that were obducted and imbricated into the Ossa-Morena Zone (Fonseca et al., 1999; Araújo et al., 2005; Ribeiro et al., 2007; 2010).

The Ossa-Morena Zone (OMZ), one of the divisions of the Iberian Terrane (IT; Fig. 1), is a distinct block accreted to the Iberian Autochthonous Terrane (IAT) during the Cadomian Cycle (Quesada, 1991; 1997; Eguiluz et al., 2000; Ribeiro et al., 2007; 2010) or the Variscan Cycle (Simancas et al., 2001; 2003; Expósito et al., 2002). It is bounded by two major tectonic sutures. To the north, the suture between OMZ and IAT corresponds to either the Tomar-Badajoz-Cordoba Shear Zone (TBCSZ), a Cadomian suture reactivated as a Variscan intraplate flower structure for some authors, or simply a Variscan suture for other authors, depending on which of the aforementioned alternative interpretations is accepted. To the south, the suture between the OMZ and the South Portuguese Terrane (SPT) corresponds to the SW-Iberia Variscan suture (Munhá et al., 1986; Quesada et al., 1994; Fonseca, 1995; Fonseca et al., 1999; Ribeiro et al., 2007; 2010), representing the closure of the Rheic and related oceans by northeastward subduction.

The western segment of the SW-Iberia Variscan suture displays imbrications of various units belonging to: (1) Neoproterozoic - Early Palaeozoic OMZ autochthonous; and (2) allochthonous complexes. The allochthonous complexes include disrupted slivers of eclogite (ca. 370 Ma; Moita et al., 2005), klippen and slices of an internal ophiolite (IOMZOS; Fonseca et al., 1999; Araújo et al., 2005; Ribeiro et al., 2010), a basal tectonic mélange (Moura Phyllonitic Complex - MPC; Araújo et al., 2005) and an external ophiolite (Beja-Acebuches Ophiolitic Complex - BAOC; Fonseca, 1995; Fonseca et al., 1999). The age of all these units is constrained by a large layered gabbroic intrusion to 350-340 Ma (Jesus et al., 2007). The BAOC (external ophiolite) is located between OMZ and SPT; it consists of a continuous thin band of metamorphosed mafic/ultramafic rocks, preserving evidence of an early obduction to the north (Fonseca, 1995). BAOC mafic rocks have Nd model ages of 380-440 Ma (Mullane, 1998) The available geochemical data indicate calk-alkaline affinities, which are symptomatic of orogenic magmatism and consistent with BAOC generation in a back-arc basin (Quesada et al., 1994; Fonseca et al., 1999). By contrast, the IOMZOS form metric to kilometric dismembered ophiolitic slices in the MPC, emplaced to the north on top of the OMZ autochthonous units. IOMZOS whole-rock geochemical data (Fonseca et al., 1999; Pedro, 2004; Araújo et al., 2005) display anorogenic affinities

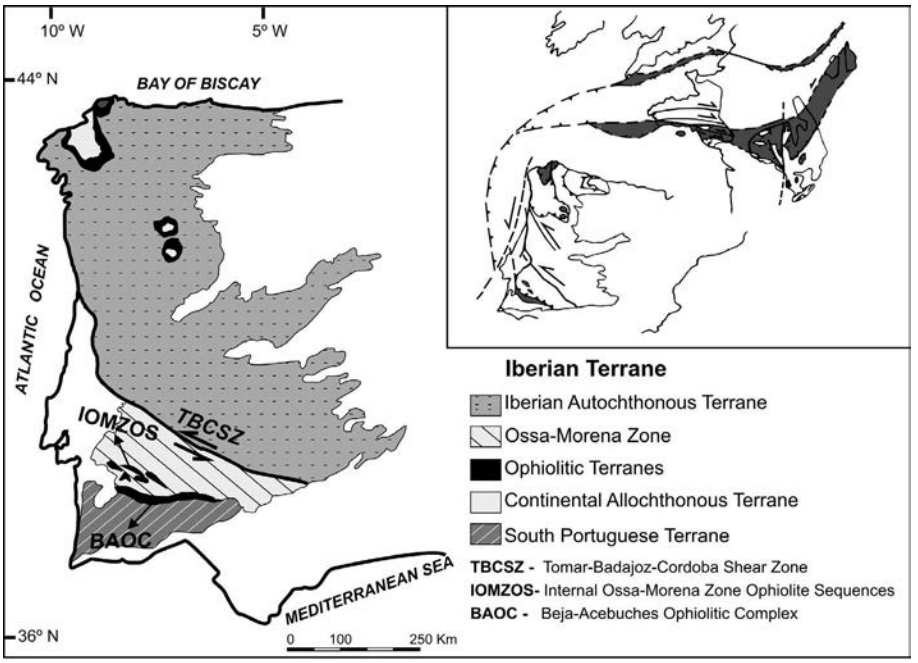

Fig. 1 - Iberian Terrane map, adapted after Ribeiro et al. (1990, 2007) and Quesada (1992). The inset shows the correlation between the Variscan sutures in Western Europe, adapted after Matte (1986). Shaded area corresponds to the innermost nappes, ophiolitic remnants and related root zones.

identical to those of mid-ocean ridge basalts (MORB-type basalts). The obduction process was recorded by both BAOC and IOMZOS and occurred in the Early-Middle Devonian (Ribeiro et al., 2007; 2010).

The recognised IOMZOS anorogenic geochemistry and internal position, in contrast to the established BAOC features, are crucial for understanding the Rheic Ocean evolution in the SW branch of the Europe Variscides Chain (Ribeiro et al., 2007; 2010). However, the IOMZOS geotectonic evolution must be analysed according to the main geodynamic events recorded in the OMZ (Eguiluz et al., 2000; Expósito et al., 2003; Sanchez-Garcia et al., 2003; Vera, 2004; Dias et al., 2006; Etxebarria et al., 2006; Quesada, 2006; Romeo et al., 2006; Ribeiro et al., 2007; 2010; Moita et al., 2009). They include: (1) a Neoproterozoic magmatic arc growth and accretion to the margin of Gondwana (Cadomian Orogeny); (2) a Cambrian-Ordovician rift event culminating with the opening of the Rheic Ocean; (3) a passive margin development during Ordovician-Early/Middle Devonian; and (4) a Late Paleozoic collisional event (Variscan Orogeny) culminating with the amalgamation of Pangea.

The OMZ Cambrian-Ordovician rifting event was recorded by large shallow plutonic and volcanic rocks accompanied by coeval sedimentary successions. Mata and Munhá (1990) and Giese and Bühn (1994) discuss a bimodal volcanism involving early acid and later basic compositions; from north to south, peralkaline rhyolites change to rhyolites, and alkali basalts change, via transitional basalts, to MOR basalts. Consistently with this model, Sanches-Garcia et al. (2003) propose an early stage of acid peraluminous volcanism followed by a main stage charactrized by the emplacement of alkaline, tholeiitic and minor calc-alkaline peraluminous rocks.

All of the above characteristics provide evidence for a significant heterogeneity during the OMZ Cambrian-Ordovician rifting processes; this may be due to the involvement of various magma sources (asthenospheric, lithospheric, and crustal) and/or the involvement of various petrogenetic processes. Moreover, this widespread bimodal rifting magmatism was diachronic and migrated from northeast (Linnemann et al., 2008) to southwest (Chichorro et al., 2008). This migration towards the SW boundary of OMZ, is interpreted as related to the onset of the Rheic Ocean opening (Ribeiro et al., 2010). However, a typical sequence of oceanic lithosphere has never been recognised in the aforementioned extensional magmatic stages rocks; consequently, they cannot be interpreted as remnants of the Rheic Ocean.

This paper aims at providing a detailed geochemical characterisation and new SHRIMP U-Pb zircon age determinations for IOMZOS, in order to show that these internal and allochthonous ophiolitic sequences in OMZ are remnants of the Rheic Ocean in SW Iberia and to facilitate the ongoing discussion on the evolution of SW Europe Variscides.

INTERNAL OSSA-MORENA ZONE OPHIOLITE SEQUENCES

Geological features

The IOMZOS consist of metric to kilometric allochthonous fragments of oceanic lithosphere, cropping out as klippens on top of and/or imbricated inside the MPC and located 50 km to the NE of the SW-Iberia Variscan suture (Fonseca et al., 1999; Pedro, 2004; Araújo et al., 2005; Pedro et al., 2005; 2006; Ribeiro et al., 2010). The IOMZOS define a narrow and discontinuous WNW-ESE belt (Fig. 2). Shear zones and related structures preserved in the IOMZOS record micro-, meso- and macroscopic kinematic indicators which indicate transport and emplacement from south to north (present day coordinates) (Araújo et al., 2005; Ribeiro et al., 2010). Greenschist/amphibolite metamorphic recrystallisation and strong Variscan deformation overprint these ophiolitic fragments and, in some cases, make the sequences incomplete and difficult to recognize. However, detailed geological mapping supported by mineralogical and petrological/geochemical data (Pedro, 2004) allowed reconstruction of the different ophiolitic units, which are always separated by shear zones. Taken as a whole, the IOMZOS fragments

preserve the typical "oceanic lithosphere pseudostratigraphy" (Fig. 3), matching those described for classic ophiolites. They include (from bottom to top): strongly serpentinised dunites and wehrlites, pyroxenite cumulates, metagabbros and flasergabbros, metagabbros intruded by metadoleritic dikes, metabasalts, and metacherts. Generally, the IOMZOS have a thin and discontinuous crustal section with sporadic stratiform pyroxenite cumulates as well as a serpentinised peridotite mantellic sequence that is often cut by pegmatoid metagabbros and metadolerite/metabasalt dikes. These features, especially the discontinuous crustal structure and the petrography of the residual mantle, led the authors to classify the IOMZOS as a Lherzolitic Ophiolite Type (Juteau and Maury, 1999). The reconstruction of an entire oceanic lithosphere cross-section in the IOMZOS is the main geological evidence that these ophiolite sequences are remnants of the Rheic Ocean in SW Iberia.

Whole-rock geochemistry and petrogenesis

All the IOMZOS units (ultrabasic and basic rock types) have been sampled in previous studies (Pedro, 2004). After petrographic examination, selected IOMZOS metabasalts and metagabbros were chosen for whole-rock geochemical analyses.

Major and trace elements analyses were performed at the Activation Laboratories - ACTLABS (Canada) using the lithium metaborate/tetraborate fusion for ICP (Code 4B) and ICP-MS (Code 4B2). Samples were fused with a flux of lithium metaborate and lithium tetraborate in an induction furnace. The melt was immediately mixed with 5% nitric acid containing an internal standard until completely dissolved. The samples were run for major and trace elements on a combination of simultaneous/sequential Thermo Jarrell-Ash ENVIRO II ICP. Calibration was performed using seven USGS and Canmet certified reference materials. One of the seven standards is used during the analysis for every group of samples. The sample solution prepared under Code 4B is spiked with internal standards to cover the entire mass range, is further diluted and is introduced into a Perkin Elmer SCIEX ELAN 6000 or 6100 ICP-MS using a proprietary (ACTLABS) sample introduction methodology. Analytical precision and accuracy for major elements are 1 to 2% and better than 5% for trace elements.

Table 1 provides 36 selected analyses (metabasaltic and metagabbroic rock types) representative of the whole IOMZOS geochemical spectrum.

Due to the effects of greenschist/amphibolite metamorphic recrystallisation, little reliance can be placed on most major elements analyses for the discussion of IOMZOS igneous petrogenesis. Under such conditions some major oxides and LOI (Loss on Ignition) should reflect the melt conditions and the metamorphic recrystallisation.

The IOMZOS metabasalts and metagabbros have SiO_2 contents ranging from 43.56 to 49.91wt% and do not show significantly different major and trace element chemical compositions. IOMZOS metabasalts display low to moderate alkali contents (Na_2O+K_2O = 1.36 to 5.02wt%) and have

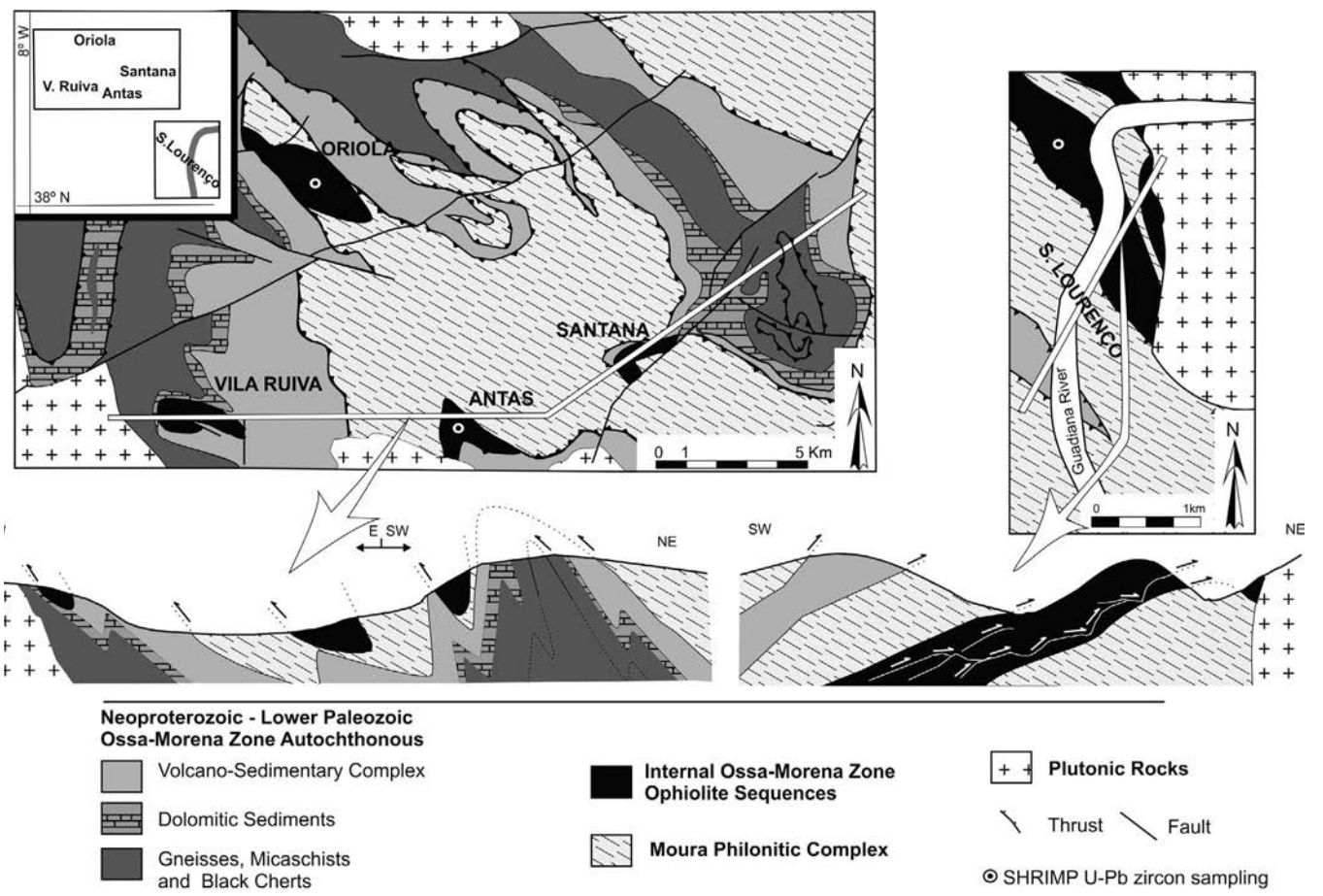

Fig. 2 - Schematic geological map and interpretative cross-section of the IOMZOS, adapted after Pedro (2004).

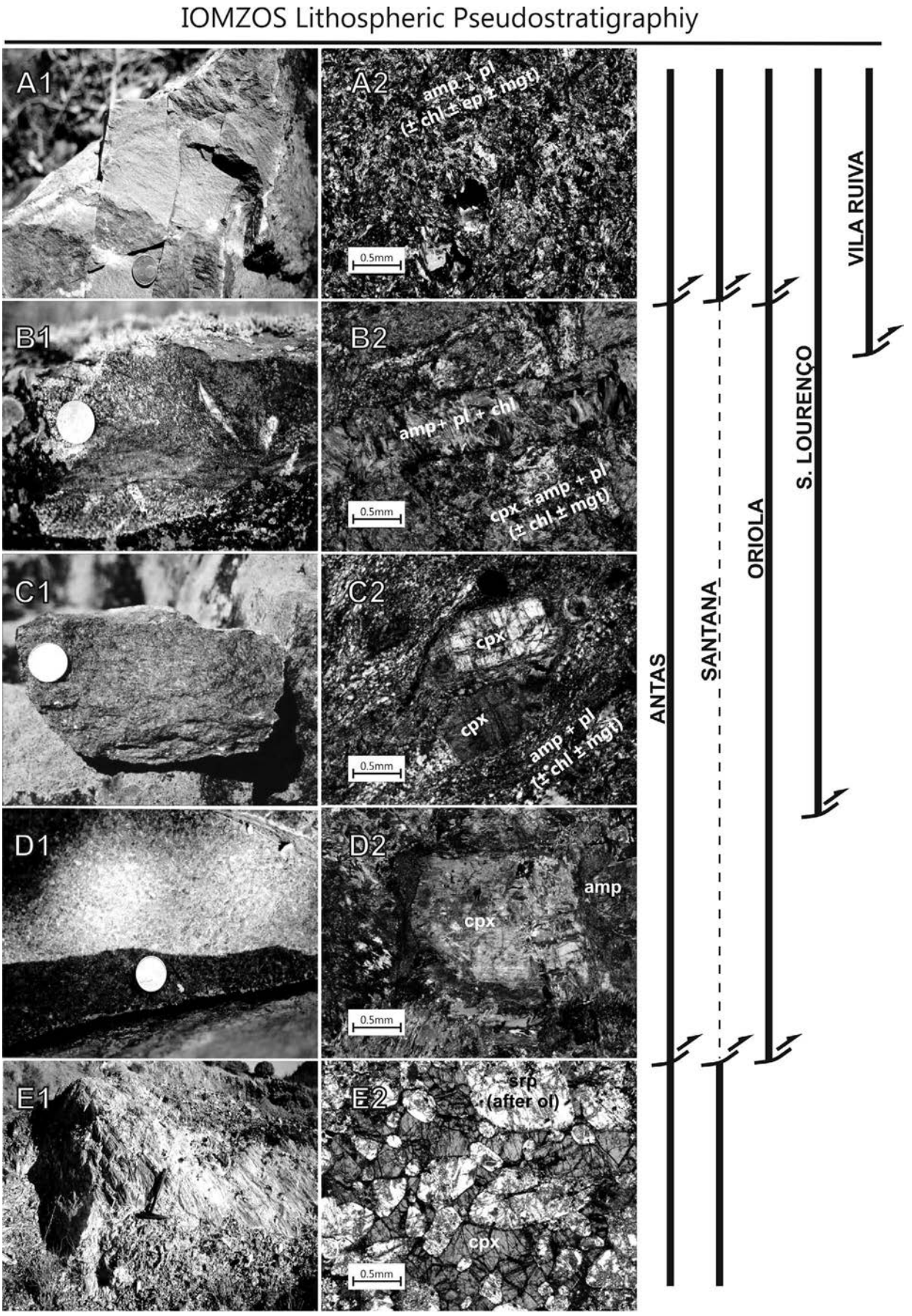

Fig. 3 - Macro- (1) and microphotographs (2) of the reconstructed lithospheric sequence in the Internal Ossa-Morena Zone Ophiolite Sequences and the main ophiolitic units in each ophiolitic fragment. A- metabasalts; B- metagabbros intruded by metadolerite dikes; C- metagabbros; D- pyroxenite cumulates; E- strongly serpentinised peridotites (dunites). amp- amphibole; chl- chlorite; cpx- clinopyroxene; ep- epidote; mgt- magnetite; srp- serpentine.

Table 1 - Major and trace element composition of metabasalts and metagabbros from the IOMZOS.

	METABASALTS																		
Outcrop	ORIOLA									ANTAS				VILA RUIVA					
	OR-4-1	OR-4-2	OR-4-3	OR-4-4	OR-4-5	OR-4-6	OR-6-1	OR-7-1	OR-8-1	ANT-1-1	ANT-1-2	ANT-1-3	ANT-2-3	VR-1-1	VR-1-2	VR-1-3	VR-1-7	VR-1-9	
Rock type	B	B	B	B	B	B	B	B	B	B	B	B	B	B	B	B	BAS	BAS	
wt. %																			
SiO_2	46,72	47,11	46,33	46,06	45,78	46,64	47,84	48,46	46,90	48,36	48,08	48,95	47,00	45,93	46,72	47,37	44,78	43,88	
TiO_2	1,02	0,94	1,22	1,00	1,19	1,06	1,74	1,92	2,15	1,99	1,55	2,09	1,59	1,98	2,05	1,95	2,13	2,33	
Al_2O_3	18,21	15,61	16,77	18,37	15,10	17,05	15,03	14,81	14,55	14,65	15,08	15,94	16,05	16,59	12,81	15,59	13,68	15,50	
$Fe_2O_3^{tot}$	8,82	10,27	10,19	8,96	10,76	10,02	12,90	12,36	12,85	10,38	11,30	10,99	10,19	9,95	12,58	9,97	11,48	11,01	
MnO	0,15	0,18	0,21	0,15	0,21	0,17	0,22	0,20	0,22	0,17	0,30	0,18	0,33	0,17	0,21	0,17	0,18	0,19	
MgO	7,65	7,71	7,22	8,17	8,85	8,18	6,91	6,09	6,83	7,08	7,07	6,30	9,28	7,91	12,75	8,53	6,01	4,74	
CaO	12,60	13,94	13,89	13,38	14,08	12,38	9,63	11,26	13,57	13,01	12,01	9,30	12,41	9,09	4,77	6,27	9,77	10,91	
Na_2O	2,96	2,33	3,03	2,15	1,83	2,79	4,17	3,78	1,19	2,05	2,22	4,18	1,86	3,40	2,26	3,63	3,11	3,65	
K_2O	0,35	0,34	0,26	0,23	0,34	0,25	0,10	0,36	0,17	0,39	0,23	0,23	0,15	0,17	0,04	0,56	0,05	0,07	
P_2O_5	0,11	0,07	0,11	0,08	0,11	0,09	0,17	0,27	0,21	0,30	0,28	0,28	0,17	0,32	0,32	0,32	0,28	0,38	
LOI	1,34	1,33	0,67	1,31	1,30	1,22	0,93	0,70	0,92	1,28	1,04	1,61	0,83	3,84	5,58	3,59	7,41	6,03	
mg #	53,21	49,61	48,16	54,46	51,89	51,70	41,26	39,25	41,07	47,21	45,07	42,91	54,43	51,04	57,06	52,87	40,71	36,08	
A.I.	0,15	0,11	0,17	0,13	0,13	0,14	0,15	0,13	0,06	0,08	0,08	0,13	0,09	0,21	0,11	0,16	0,30	0,72	
ppm																			
Y	16,0	21,0	25,0	20,0	23,0	21,0	35,0	24,0	39,0	33,5	22,6	33,2	26,2	24,0	28,7	23,6	30,5	28,5	
Zr	59	46	71	53	61	55	109	149	137	143	114	149	96	146	149	143	160	171	
Nb	4,70	1,80	1,80	2,40	5,20	2,10	5,50	16,00	8,10	22,70	22,70	19,70	6,10	22,23	21,92	21,56	12,90	24,61	
La	4,20	2,03	2,68	2,56	4,61	2,26	5,81	12,80	7,88	19,80	19,30	15,40	4,06	16,20	17,53	15,52	13,59	19,70	
Ce	10,50	5,88	8,51	7,24	11,00	6,90	15,40	30,10	20,40	43,30	40,50	37,00	12,90	34,17	37,51	33,20	31,49	41,76	
Pr	1,41	0,97	1,33	1,15	1,58	1,15	2,32	3,83	2,99	5,04	4,52	4,47	1,90	3,90	5,01	3,83	3,88	4,89	
Nd	7,72	5,95	8,65	6,86	8,98	7,14	13,20	18,70	16,90	23,00	19,60	20,70	10,30	18,15	21,46	17,79	18,59	22,48	
Sm	2,24	2,19	3,06	2,31	2,84	2,54	4,11	4,58	5,17	5,62	4,26	5,27	3,15	4,47	5,60	4,24	5,01	5,51	
Eu	0,85	0,84	1,21	0,93	1,21	0,98	1,54	1,36	1,83	1,93	1,50	1,85	1,09	1,51	1,91	1,47	1,81	1,88	
Gd	3,08	2,93	3,92	2,98	3,52	3,28	5,21	4,62	6,28	5,97	4,35	6,09	4,03	4,54	5,54	4,60	5,35	5,74	
Tb	0,54	0,61	0,77	0,62	0,71	0,67	1,04	0,85	1,24	1,05	0,71	1,06	0,74	0,71	0,94	0,70	0,86	0,91	
Dy	3,30	3,82	4,87	3,83	4,46	4,09	6,44	4,90	7,43	6,32	4,15	6,24	4,74	4,21	5,78	4,12	5,34	5,09	
Ho	0,67	0,81	1,03	0,79	0,89	0,86	1,34	0,98	1,55	1,25	0,81	1,26	1,03	0,84	1,18	0,85	1,11	1,04	
Er	2,04	2,48	3,02	2,41	2,72	2,58	4,13	2,95	4,61	3,59	2,50	3,73	3,12	2,46	3,44	2,39	3,21	2,97	
Tm	0,29	0,36	0,44	0,34	0,39	0,37	0,58	0,41	0,67	0,53	0,35	0,54	0,47	0,34	0,48	0,33	0,44	0,40	
Yb	1,84	2,30	2,69	2,13	2,39	2,33	3,67	2,59	4,17	3,25	2,18	3,19	2,90	2,06	3,15	1,98	2,77	2,47	
Lu	0,27	0,34	0,40	0,32	0,36	0,35	0,56	0,38	0,62	0,48	0,33	0,49	0,46	0,29	0,45	0,28	0,39	0,34	
Hf	1,60	1,40	2,00	1,50	1,90	1,70	3,00	3,70	3,70	3,60	2,80	3,70	2,60	3,30	3,86	3,19	3,62	4,08	
Ta	0,29	0,10	0,08	0,13	0,31	0,11	0,34	0,99	0,49	1,42	1,64	1,10	0,17	1,72	1,55	1,65	0,99	1,91	
Th	0,36	0,14	0,11	0,17	0,38	0,15	0,38	1,12	0,56	1,65	1,96	1,22	0,22	1,44	1,77	1,40	0,91	1,70	
$(La/Sm)_{CN}$	1,21	0,60	0,57	0,72	1,05	0,57	0,91	1,80	0,98	2,27	2,92	1,89	0,83	2,34	2,02	2,36	1,75	2,31	
$(La/Yb)_{CN}$	1,64	0,63	0,71	0,86	1,38	0,70	1,14	3,54	1,36	4,37	6,35	3,46	1,00	5,64	3,99	5,61	3,52	5,71	

	METABASALTS																METAGABBROS		
Outcrop	VILA RUIVA			SANTANA				S. LOURENÇO									ORIOLA	ANTAS	S. LOURENÇO
	VR-1-10	VR-1-11	VR-1-18	SAT-1	SAT-4	SAT-7	SAT-8	AF-12	AF-13	AF-14	AF-15	AF-18	AF-20	AF-21	AF-22		OR-1-2	ANT-1-7	AF-3
Rock type	BAS	BAS	BAS	B	PB	B	B	B	BAS	B	B	B	B	B	B		GN	HG	HG
wt. %																			
SiO_2	45,08	44,63	43,56	49,14	44,07	48,69	49,91	45,75	44,22	45,47	46,08	48,42	48,49	49,45	49,27		48,63	46,69	47,63
TiO_2	2,09	1,96	2,34	2,47	2,07	2,12	2,03	1,71	1,72	1,64	1,99	1,44	2,04	1,43	1,91		1,63	1,41	1,35
Al_2O_3	17,25	14,77	14,96	13,52	15,36	15,26	14,93	19,03	18,85	16,88	14,92	16,45	14,77	15,92	16,76		9,57	16,20	17,81
Fe_2O_3	10,28	9,83	10,90	12,99	13,93	11,41	11,10	9,79	8,96	9,00	9,98	10,55	12,54	9,83	10,83		12,09	8,77	8,49
MnO	0,18	0,21	0,24	0,19	0,28	0,20	0,21	0,14	0,14	0,14	0,17	0,15	0,28	0,16	0,18		0,22	0,15	0,17
MgO	7,84	6,25	7,36	5,81	7,36	5,18	5,27	4,68	5,87	4,49	4,57	9,48	7,49	8,31	6,52		10,35	7,96	6,71
CaO	8,45	7,80	6,81	6,55	7,70	9,36	8,76	10,75	10,99	11,77	13,14	7,53	10,48	7,38	9,86		13,72	10,81	11,37
Na_2O	3,53	3,64	3,45	3,26	2,58	3,56	3,88	3,93	3,50	2,85	3,44	4,30	2,88	4,84	3,88		1,73	3,00	3,27
K_2O	0,17	0,49	0,32	0,60	0,25	0,25	0,29	0,10	0,10	0,16	0,08	0,04	0,30	0,18	0,20		0,22	0,44	0,08
P_2O_5	0,41	0,32	0,35	0,32	0,21	0,26	0,28	0,26	0,24	0,24	0,28	0,18	0,20	0,14	0,24		0,14	0,21	0,20
LOI	4,15	8,56	9,29	4,56	5,16	2,61	2,46	4,38	5,29	6,63	7,12	2,43	0,92	2,08	1,30		0,97	1,99	2,06
mg #	50,00	45,47	46,96	36,97	40,93	37,32	38,37	38,53	46,21	39,55	37,52	54,09	43,92	52,57	44,12		52,89	54,34	50,89
A.I.	0,30	0,43	1,14	0,11	0,45	0,11	0,10	0,25	0,50	0,21	0,19	0,14	0,10	0,13	0,11		0,06	0,16	0,12
ppm																			
Y	25,7	32,6	34,9	39,0	35,7	31,4	30,1	26,0	24,0	22,0	28,0	24,0	32,0	26,0	30,0		29,00	22,57	22,00
Zr	150	160	157	173	127	152	145	138	133	125	147	114	132	103	147		83,00	93,17	110,00
Nb	23,12	16,22	23,70	9,12	5,23	9,35	9,07	7,70	7,80	7,20	8,30	3,00	3,60	2,20	7,90		4,10	10,74	6,20
La	16,73	14,93	19,68	9,73	6,86	9,81	9,40	9,70	9,40	8,80	10,40	5,80	8,20	3,60	11,00		4,44	9,28	7,40
Ce	35,72	32,88	41,08	25,79	18,27	25,44	24,35	22,00	22,00	22,00	25,00	16,00	23,00	11,00	26,00		12,50	20,61	18,00
Pr	4,11	3,96	4,79	3,49	2,52	3,32	3,20	n d	n d	n d	n d	n d	n d	n d	n d		1,83	2,48	n d
Nd	19,11	19,02	22,31	18,27	13,67	16,98	16,27	14,00	13,00	13,00	15,00	11,00	16,00	10,00	16,00		10,80	11,90	12,00
Sm	4,66	4,94	5,66	5,26	4,35	4,68	4,55	3,80	3,70	3,50	4,30	3,10	4,00	2,90	4,00		3,61	3,22	3,10
Eu	1,64	1,70	1,77	1,95	1,69	1,72	1,65	1,40	1,36	1,29	1,40	1,13	1,49	1,22	1,58		1,22	1,19	1,14
Gd	4,93	5,47	6,11	6,05	5,02	5,16	4,98	n d	n d	n d	n d	n d	n d	n d	n d		5,20	3,56	n d
Tb	0,74	0,90	0,99	1,06	0,94	0,88	0,85	0,80	0,80	0,80	0,90	0,80	0,80	0,70	0,90		0,95	0,61	0,70
Dy	4,42	5,46	5,96	6,66	5,98	5,42	5,28	n d	n d	n d	n d	n d	n d	n d	n d		5,85	3,79	n d
Ho	0,90	1,19	1,29	1,41	1,31	1,16	1,12	n d	n d	n d	n d	n d	n d	n d	n d		1,24	0,83	n d
Er	2,56	3,55	3,69	4,06	3,85	3,27	3,18	n d	n d	n d	n d	n d	n d	n d	n d		3,74	2,32	n d
Tm	0,35	0,49	0,53	0,56	0,55	0,47	0,45	n d	n d	n d	n d	n d	n d	n d	n d		0,55	0,33	n d
Yb	2,18	3,01	3,24	3,53	3,37	2,84	2,81	2,46	2,41	2,31	2,75	2,23	2,95	2,43	2,98		3,46	2,04	2,06
Lu	0,31	0,43	0,46	0,50	0,49	0,38	0,37	0,39	0,38	0,38	0,43	0,35	0,44	0,38	0,40		0,52	0,30	0,33
Hf	3,40	3,78	3,76	4,06	3,21	3,45	3,34	2,80	2,80	2,70	3,10	2,40	2,90	2,10	3,10		2,40	2,18	2,30
Ta	1,63	1,22	1,78	0,72	0,46	0,80	0,68	0,80	0,70	1,00	0,80	0,50	0,70	0,30	0,90		0,24	0,87	0,50
Th	1,45	1,11	2,22	0,61	0,35	0,61	0,60	0,70	0,80	0,70	0,90	0,50	0,50	0,20	0,80		0,37	0,75	0,60
$(La/Sm)_{CN}$	2,32	1,95	2,25	1,20	1,02	1,35	1,33	1,65	1,64	1,62	1,56	1,21	1,32	0,80	1,78		0,79	1,86	1,54
$(La/Yb)_{CN}$	5,51	3,56	4,35	1,98	1,46	2,48	2,40	2,83	2,80	2,73	2,71	1,87	1,99	1,06	2,65		0,92	3,26	2,58

Rock type after Le Maitre et al. (1989): B-basalt, BAS-basanite, PB-picrobasalt, GN-gabbronorite, HG-horneblende gabbro.

Data determined by ICP-MS at Activation Laboratoires Lda - Canada.

FeO recalculated from $Fe_2O_3^{tot}$ according to Middlemost (1989).

A.I. = $[(Na_2O + K_2O) / (SiO_2 - 43) * 0.17]$

mg # = 100*[MgO / (MgO + FeO)]

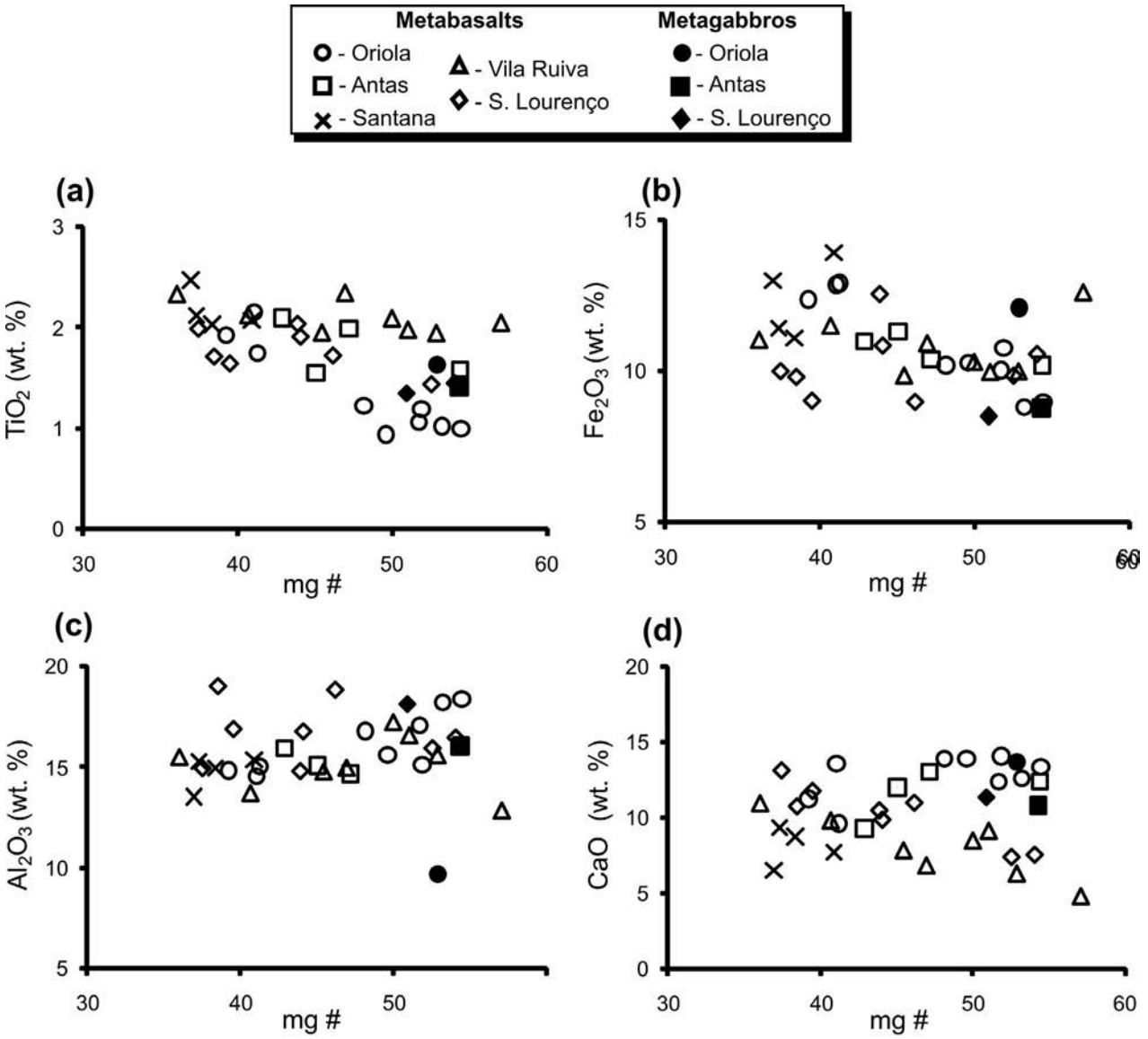

Fig. 4 - Major elements variations for the IOMZOS metabasic rocks: (a) TiO_2; (b) $Fe_2O_3^{tot}$; (c) Al_2O_3 and (d) CaO against mg#.

basaltic and basanitic compositions, whereas the metagabbros (Na_2O+K_2O = 1.95 to 3.44wt%) are gabbros s.s. (Le Bas et al., 1986). The Na_2O (1.19-4.84wt%) and K_2O (0.04-0.60wt%) variations are transitional between the alkalic and sub-alkalic basalts (Middlemost, 1975; Wilson, 1989) while the Alkali Index (0.06-1.14) and Al_2O_3 contents (9,57-19.03wt%) suggest tholeiitic affinities for the IOMZOS metabasic rocks (Middlemost, 1975).

As shown in Fig. 4 the IOMZOS metabasic rocks display considerable variations in the major elements against the mg# values. The $Fe_2O_3^{tot}$ (Fig. 4a) and TiO_2 (Fig. 4b) data have a general tendency for negative correlation although the Al_2O_3 (Fig. 4c) exhibits a slight positive correlation. The CaO plot (Fig. 4d) reveals some dispersion in the data, which reflects the modal abundances of metamorphic paragenesis (i.e. epidote, actinolite, actinolitic hornblende) present in the IOMZOS metabasic rocks. The observed trends with decrease of Al_2O_3 and mg# with TiO_2 and $Fe_2O_3^{tot}$ increase, without a significant variation in SiO_2, suggest that plagioclase fractionation was important in the IOMZOS metabasalts and metagabbros evolution. Such relationships are common in magmatic tholeiitic series (Miyashiro, 1974) and support a tholeiitic affinity for the IOMZOS igneous protoliths. Sun and Nesbitt (1978) discussed the genetic significance of basalts associated with ophiolitic complexes using Al_2O_3 and TiO_2 variations and pointed out that ophiolitic basalts derived from MORB-type magmas have high Ti contents (TiO_2>0.7%). This assumption allows the classification of the IOMZOS metabasalts as high-Ti basalts and suggests that they evolved from MORB-type magmas.

In general, the variations in trace elements of metamorphic rocks seem more reliable indicators of their igneous petrogenesis than the major elements variations. The HFSE (High Field Strength Elements) like REE, Th, Nb, Ta, Zr, Hf, Ti, Y, etc. are believed to be relatively immobile during metamorphism, alteration and sea-floor alteration (Pearce and Cann, 1973; Pearce, 1982; 1983; Rollinson, 1993) and should reflect primary igneous characteristics. Therefore, the IOMZOS geochemical analysis and subsequent petrogenetic interpretation will be based on the HFSE geochemical variations.

The IOMZOS metabasalts and metagabbros concentrations of Th (0.8±0.6 ppm), Nb (10.7±0.2 ppm) , Ta (0.8±0.5 ppm), Zr (122.2±36.3 ppm), Hf (2,9±0.8 ppm), Ti (10468±2485 ppm) and Y (27.5±5.6 ppm) are comprised within the range of ocean-floor tholeiites (Pearce and Cann, 1973; Wood, 1980; Sun and McDonough, 1989) in accordance with the tholeiitic affinities suggested by the major elements.

The variations in incompatible element ratios (Pearce and Cann, 1973), like Ti/Zr (88.7±13.1) and Zr/Y (4.4±1.1), and the appropriate diagrammatic representation, such as the Th-Hf-Ta discriminating diagram (after Wood, 1980; Fig. 5), support the tholeiitic affinity of IOMZOS metabasic rocks. The data in Fig. 5 show an affinity between the IOMZOS metabasic rocks and anorogenic oceanic basalts, ranging from N-MORB (less enriched) to Alkaline Within-Plate Basalts (more enriched) and do not suggest any orogenic geochemical signature for the IOMZOS metabasic rocks. This anorogenic geochemical fingerprint of IOMZOS metabasic rocks is also well defined in the La vs. Nb (Fig. 6a) and La vs. Th (Fig. 6b) diagrams (after Gill, 1981). The plotted data show strong positive correlations between these pairs of elements (La/Nb = 1.08±0.3; La/Th = 13.68±3.1), with a coherent and progressive enrichment in both LILE (Large Ion Lithophile Elements) and HFSE and without the typical LILE/HFSE decoupling observed in many orogenic basalts (Gill, 1981; Pearce, 1982, 1983; Wilson, 1989; Miyashiro, 1994; Juteau and Maury, 1999). The presented data define a geochemical transitional MORB (T-MORB) fingerprint for the IOMZOS metabasic rocks, with abundances and ratios between the reported values in the normal (N-MORB) and enriched (E-MORB) mid-oceanic ridge basalts (Sun et al., 1979; Sun, 1980; Gill, 1981; Wilson, 1989; Flower, 1991; Miyashiro, 1994; Juteau and Maury, 1999). Moreover, the low La/Nb (<2) and high La/Th (>10) ratios of the metabasic rocks of the IOMZOS are consistent with the reported values for asthenospheric mantle (Sun and McDonough, 1989; Green, 1995; Pearce, 2008) which provides an argument for derivation of the IOMZOS igneous protoliths from an asthenospheric mantle source.

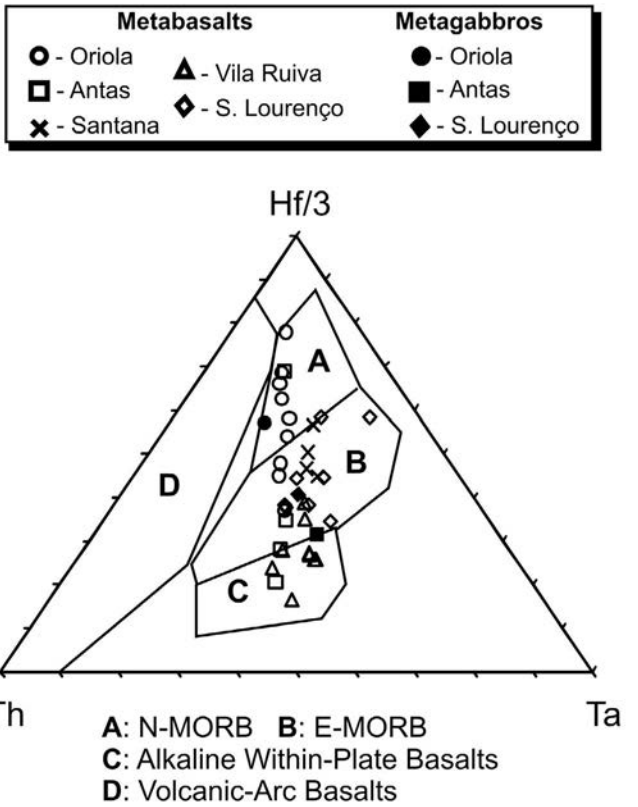

Fig. 5 - Th-Hf-Ta ternary diagram (after Wood, 1980) for the IOMZOS metabasic rocks.

Chondrite-normalised trace element multivariation and

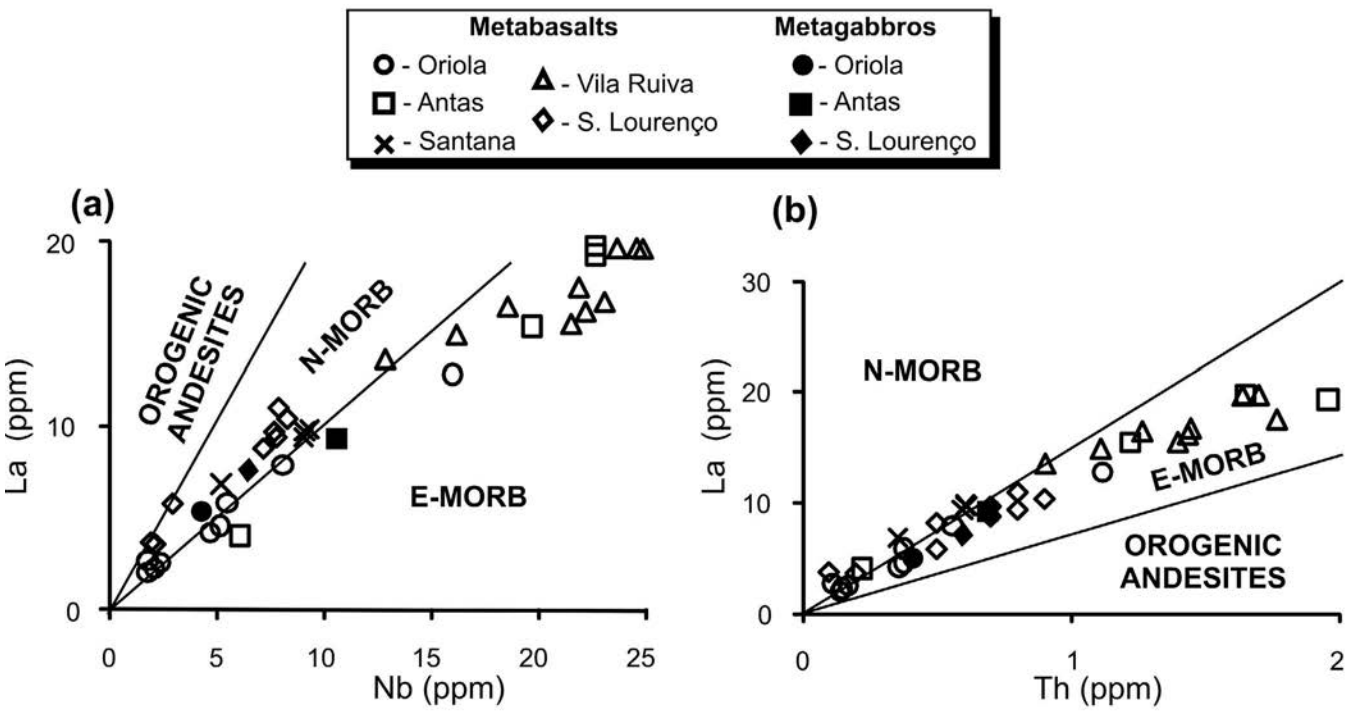

Fig. 6 - (a) La vs. Nb and (b) La vs Th diagrams (after Gill, 1981) for the IOMZOS metabasic rocks.

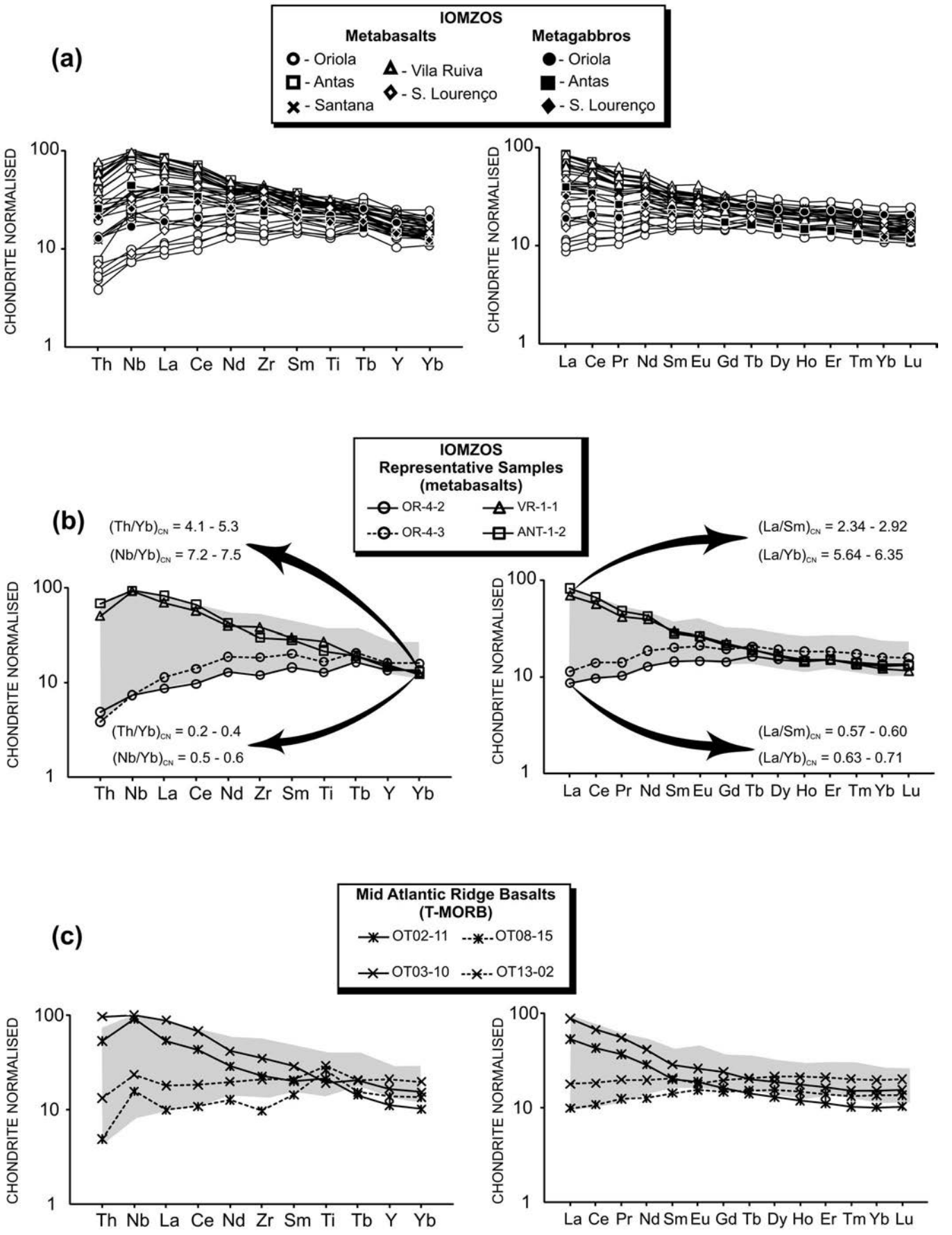

Fig. 7 - Trace element multivariation and REE chondrite-normalised diagrams: (a) IOMZOS metabasic rocks; (b) IOMZOS representative metabasalts; and (c) present-day Mid Atlantic Ridge Basalts. Shaded field represents the IOMZOS variations. Normalised values after Sun et al. (1979), Sun and Nesbitt (1977) and Sun and McDonough (1989). Mid Atlantic Ridge Basalts data after Niu et al. (2001).

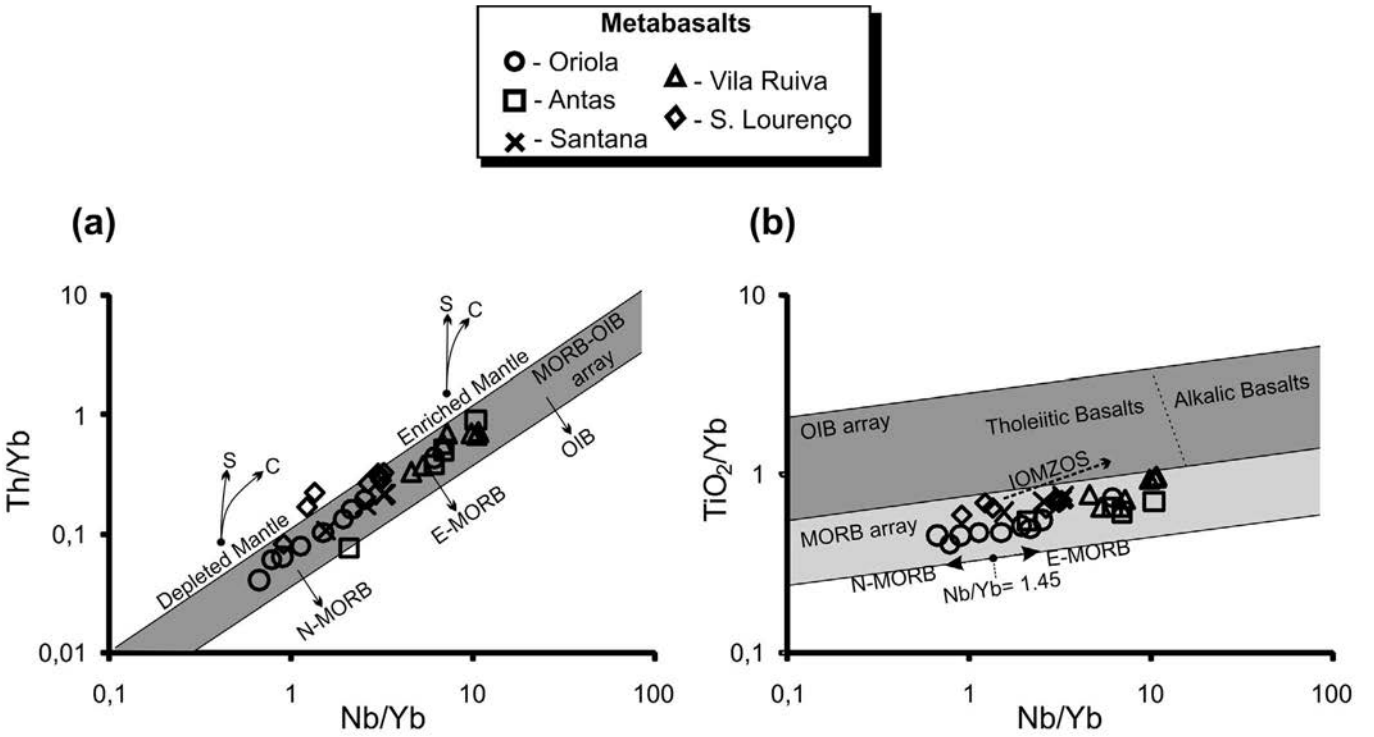

Fig. 8 - (a) Th/Yb vs. Nb/Yb and (b) TiO_2/Yb vs. Nb/Yb diagrams (after Pearce, 2008) for the IOMZOS metabasalts. Arrows show the influence of subduction components (S) and crustal contamination (C). OIB - Ocean island basalts.

REE diagrams are presented in Fig. 7. The data show different patterns for the IOMZOS metabasic rocks (Fig. 7a) covering the entire and typical MORB suite (Sun et al., 1979; Sun, 1980; Wilson, 1989). Despite the overload data plot on Fig. 7a, two main IOMZOS patterns (Fig. 7b), including the samples with lower (metabasalts OR-4-2 and OR-4-3) and higher (metabasalts ANT-1-2 and VR-1-1) Th/Yb, Nb/Yb, La/Sm and La/Yb ratios, are representative of the overall IOMZOS geochemistry. Samples OR-4-2 and OR-4-3 present similar patterns to those commonly reported for N-MORB (Sun et al., 1979; Sun, 1980; Wilson, 1989). They are slightly depleted in LREE with respect to MREE an HREE [$(La/Sm)_{CN}$ = 0.57 to 0.60, $(La/Yb)_{CN}$ = 0.63 to 0.71 and Yb_{CN} contents 14-16 times those in chondrite]. The LREE are somewhat enriched relative to Nb and Th [$(La/Nb)_{CN}$ = 1.17 to 1.55 and $(La/Th)_{CN}$ = 1,77 to 2.98] while Th and Nb are depleted relative to Zr and Ti. On the contrary, samples ANT-1-2 and VR-1-1 display patterns correlated with E-MORB (Sun et al., 1979; Sun, 1980; Wilson, 1989). They are considerably enriched in the more incompatible elements (Th, Nb, La and Ce) relative to less incompatible elements (Zr, Ti, Y and Yb). The LREE are enriched relatively to MREE and HREE [$(La/Sm)_{CN}$ = 2.34 to 2.92, $(La/Yb)_{CN}$ = 5.64 to 6.35 and Yb_{CN} contents 12-13 times those in chondrite) and Nb is enriched with respect to Th and La [$(La/Nb)_{CN}$ = 0.76 to 0.88 and $(Th/Nb)_{CN}$ = 0.55 to 0.73]. The remaining IOMZOS samples display patterns intermediate between the above mentioned patterns, without any HFSE (Nb) negative anomaly; they are transitional between N-MORB and E-MORB. Fig. 7c illustrates five present-day Mid Atlantic Ridge Basalts, with typical T-MORB geochemistry (Niu et al., 2001), and shows their great geochemical similarity with the IOMZOS metabasic rocks. Therefore, the overall IOMZOS whole-rock geochemistry is consistent with T-MORB geochemistry, ranging from N-MORB to E-MORB, and supports the anorogenic tholeiitic geochemical fingerprint previously proposed for the igneous protoliths.

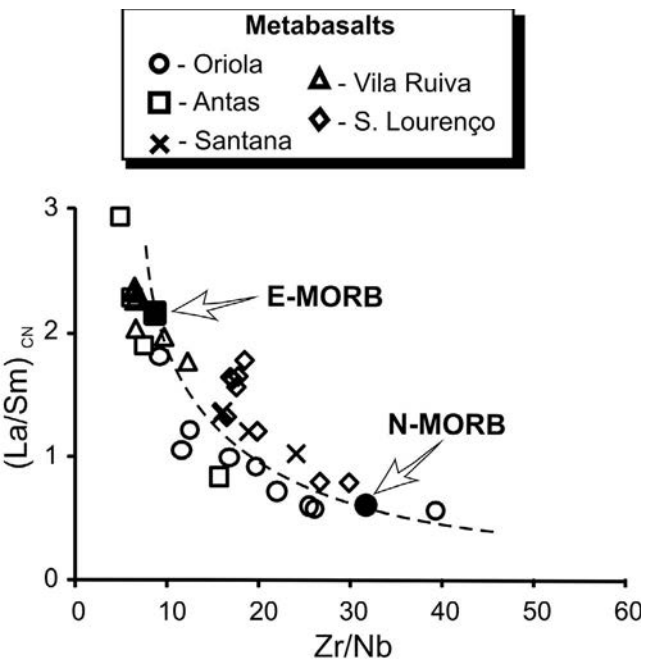

Fig. 9 - $(La/Sm)_{CN}$ vs. Zr/Nb diagram for the IOMZOS metabasalts. The dashed line illustrates the expected compositional variation between E-MORB and N-MORB. MORB data from Sun et al. (1979), and Sun and McDonough (1989).

The IOMZOS whole-rock geochemistry requires magma differentiation to explain the observed geochemical heterogeneities. The compositional variations in Fig. 4 suggest that the IOMZOS metabasic rocks underwent low pressure fractional crystallization but it cannot explain all the geochemical variations observed in the IOMZOS metabasalts.

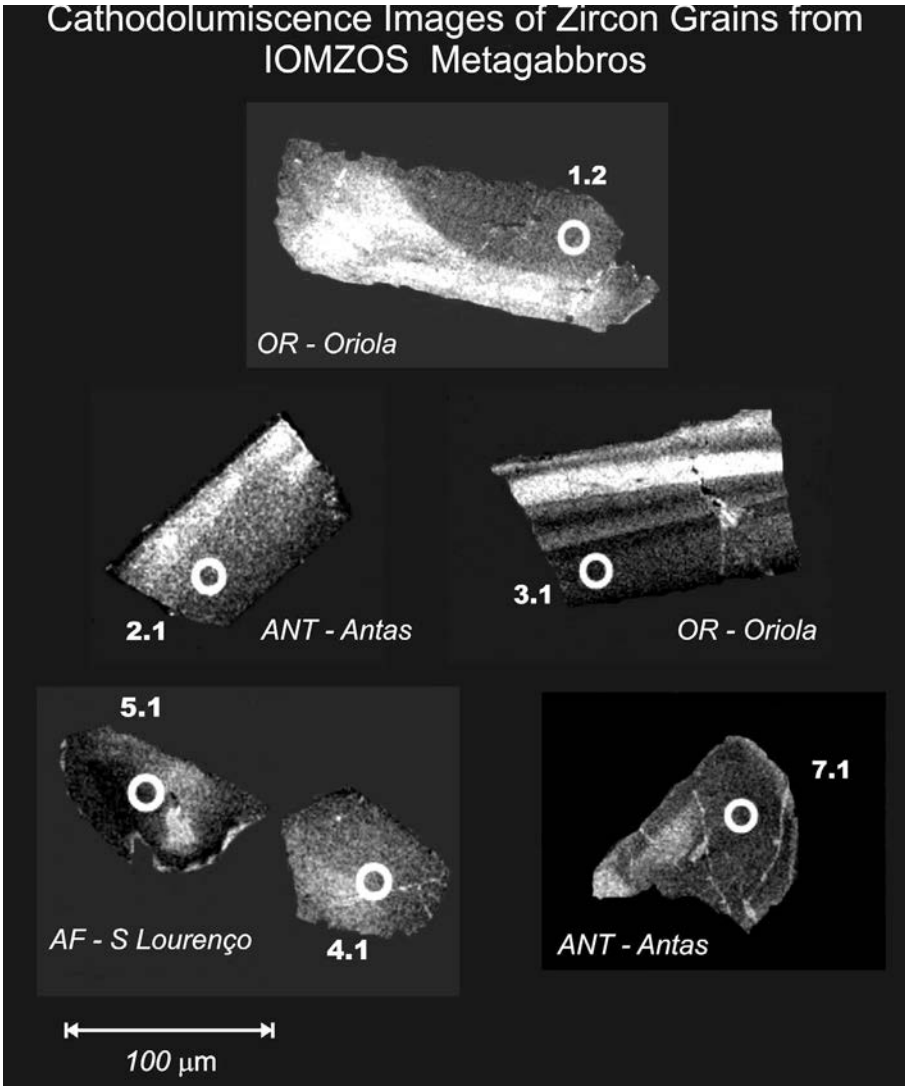

Fig. 10 - Zircon cathodoluminescence images and SHRIMP spot analyses locations.

Table 2 - SHRIMP zircon U-Pb isotopic data of the IOMZOS metagabbros.

Outcrop	Sample	spot	$^{206}Pb_c$ [%]	U [ppm]	Th [ppm]	Th/U	$^{232}Th/^{238}U$	$^{206}Pb^*$ [ppm]	$^{207}Pb^*/^{206}Pb^*$ [%]	±	$^{207}Pb^*/^{235}U$ [%]	±	$^{206}Pb^*/^{238}U$ [%]	±	Age $^{206}Pb^*/^{238}U$ [Ma]	±
Oriola	OR-1-2	1.2	0,72	268	326	1,22	1,26	17,90	0,0561	4,7	0,599	4,8	0,07745	1,0	480,9	4,8
		3.1	1,37	194	234	1,21	1,25	12,90	0,0531	7,3	0,558	7,4	0,07626	1,3	473,7	5,8
Antas	ANT-1-7	2.1	0,19	136	143	1,05	1,08	9,01	0,0580	3,8	0,616	4,0	0,07710	1,4	478,8	6,3
		7.1	0,71	215	221	1,03	1,06	14,20	0,0537	4,1	0,567	4,3	0,07667	1,2	476,2	5,3
S. Lourenço	AF-3	4.1	0,38	118	301	2,55	2,64	8,09	0,0628	4,8	0,688	5,0	0,07940	1,5	492,3	7,0
		5.1	0,23	170	182	1,07	1,11	11,70	0,0573	3,3	0,634	3,5	0,08020	1,3	497,5	6,1

Errors are 1σ; Pb_C and Pb* indicate the common and radiogenic portions, respectively;
Common Pb corrected using measured ^{204}Pb.

To generate the REE patterns [$(La/Yb)_{CN}$ = 5.64 to 6.35] and Th (1.44-1.96 ppm) contents of samples ANT-1-2 and VR-1-1 from a parent magma having a composition similar to samples OR-4-2 and OR-4-3 [$(La/Yb)_{CN}$ = 0.63 to 0.71 and Th = 0.14 to 0.11 ppm), very large amounts of (clinopyroxene dominated) crystallization (F<0.10) would be required, which is inconsistent with their contents of major and trace elements. In order to reduce the mineral accumulation effect, the IOMZOS igneous petrogenetic interpretation will be based only on the metabasalts whole-rock geochemistry, where the effects of crystal accumulation are absent. However, the IOMZOS metagabbros and metabasalts obviously lack significant geochemical differences.

As previously discussed, low La/Nb and high La/Th ratios suggest asthenospheric mantle sources for the IOMZOS protoliths. If partial melting is somehow extensive (F>0.10) the high incompatible elements should not be fractioned one from another and the REE ratios should reflect those of the mantle source (Wilson, 1989). Nevertheless, in the most evolved IOMZOS metabasalts (e.g., ANT-1-2 and VR-1-1) the Sm/Yb (1.95 to 2.17) and Lu/Hf (0.12 to 0.09) ratios are fractioned with an enrichment in Sm and Hf relative to Yb and Lu. Sm and Hf are incompatible elements, with identical partition coefficients, in mantle peridotites, while Yb

and Lu are highly compatible elements in garnet (Rollinson, 1993). Therefore, the specified fractionation between Sm/Yb and Lu/Hf, detected in the IOMZOS metabasalts, is due to the presence of residual garnet in the IOMZOS asthenospheric source (garnet lherzolite).

The partial melting effect, from the same garnet lherzolite asthenospheric source (e.g. 55% olivine + 25% orthopyroxene + 15% clinopyroxene + 5% garnet), on the IOMZOS REE geochemical variations (i.e. Ce/Yb vs. Ce) requires minimum degrees of partial melting (F<0.03) for the ANT-2-1 and VR-1-1 metabasalts (Ce/Yb = 16.6 to 18.6 and Ce = 34.17 to 40.50), whereas the OR-4-2 and OR-4-3 (Ce/Yb = 2.56 to 3.16 and Ce = 5.88 to 8.51) requires extensive partial melting (F = 0.25 to 0.30), although the large observed variations in La/Ce (0.31 to 0.47), La/Nb (0.73 to 1.49) and La/Th (9.85 to 24.36) ratios in these samples could not be generated by such process. Consequently, partial melting would only have a negligible effect on the high incompatible elements variations and this supports the existence of heterogeneities in the IOMZOS asthenospheric mantle source.

The systematic variations like Th/Yb vs. Ta/Yb (Pearce, 1982; 1983) and Th/Yb vs. Nb/Yb (Pearce and Peate, 1995; Pearce, 2008) have been successfully used to detect the characteristics of the mantle sources of oceanic basalts. The use of incompatible elements ratios, with a common denominator (Yb), has the effect of removing the variations due to partial melting and fractional crystallization processes, focusing on source composition as the main petrogenetic variable. Pearce (2008) proposed a combined methodology [(Th/Yb vs. Nb/Yb)-(TiO_2/Nb vs. Nb/Yb)] in order to highlight source and melt effects, crustal contamination and garnet residue on oceanic metabasalts. On the Th/Yb vs. Nb/Yb diagram (after Pearce, 2008; Fig. 8a), despites two anomalous samples (analytical error?), the IOMZOS metabasalts plot inside the MORB-OIB (Ocean Island Basalts) array, near the upper boundary and does not suggest any lithospheric contamination (high Th/Yb). Likewise, the Th/Yb (0.31±0.24) and Ta/Yb (0.32±0.24) ratios are also in accordance with the established trend and they do not reveal any anomalous sample. Consequently, the Th/Yb and Nb/Yb (or Ta/Yb) variations indicate that the IOMZOS mantle source(s) was heterogeneous (transitional between the N- and E-MORB sources), does not have subduction influence and the resulting magmas were not affected by any significant lithospheric contamination.

In order to better constrain the IOMZOS mantle source, the TiO_2/Yb vs. Nb/Yb variation diagram (after Pearce, 2008) of Fig 8b presents the IOMZOS metabasalts data along the MORB array with a tenuous crosswise trend, from the MORB array to the tholeiitic OIB field, suggesting the presence of garnet residues during melting (relative enrichment in TiO_2 and Nb; Pearce, 2008). Moreover, this fact together with the IOMZOS mantle source features inferred from the Th/Yb and Nb/Yb variations, are coherent with the plume/proximal ridge interactions (Pearce, 2008). In addition, a plume/ridge interaction is also supported by the $(La/Sm)_{CN}$ vs. Zr/Nb variations (Fig. 9), corroborating the above mentioned IOMZOS geochemical features. The IOMZOS mantle source(s) heterogeneity results from binary mixing between two final end-members: (1) an enriched member, similar to the E-MORB mantle source, with $(La/Sm)_{CN}$>2 and Zr/Nb<10; and (2) a depleted member, similar to the N-MORB mantle source, with $(La/Sm)_{CN}$<1 and Zr/Nb>30.

According to the presented data, and despite the negligible effect of fractional crystallization and small variations in partial melting degree, the mantle source heterogeneity is interpreted as the foremost petrogenetic variable in IOMZOS petrogenesis. Indeed, the anorogenic tholeiitic geochemistry of the IOMZOS, transitional between N-MORB and E-MORB, is analogous to the chemistry observed in many present-day ocean-floor basalts (Wilson, 1989; Floyd, 1991; Juteau and Maury, 1999; Hannigan et al., 2001; Niu et al., 2001, Roux et al., 2002; Pearce, 2008), indicating that the igneous protoliths of IOMZOS are genetically related to ocean basins and have no orogenic influence and/or crustal contamination in their petrogenesis. Moreover, based on Th/Yb, Nb/Yb and TiO_2/Yb variations, the IOMZOS tectonomagmatic evolution can be linked to modern analogues, like the Red Sea and the South America-Antarctic ridge (Pearce, 2008) and is in total accordance with the stages of the OMZ Cambrian-Ordovician rift evolution (Ribeiro et al., 2007; 2010). Several extensional magmatic stages were often proposed for the OMZ Cambrian-Ordovician rifting evolution, invoking asthenospheric, lithospheric, and crustal magma sources (Sanchez-Garcia et al., 2003; Chichorro et al., 2008; Linneman et al., 2008). Nevertheless, these stages should symbolize only the initial rifting stages (primary budding stages), while the IOMZOS record an early/full divergent margin stage of the Rheic Ocean evolution, preserved in SW Iberia by obduction. This interpretation is supported by the following IOMZOS geological and whole-rock geochemical features: (1) presence of an oceanic lithosphere sequence like Lherzolitic Ophiolite Type (related to slow spreading centers; Juteau and Maury, 1999); (2) considerable amounts of serpentinised peridotites (recording sea-floor metamorphism; Pedro, 2004); (3) magma generation related to plume-proximal ridge system (asthenospheric source); and (4) recognition of modern geochemical analogues (Red Sea and South America-Antarctic ridge, both related to slow spreading centers; Pearce, 2008).

SHRIMP U-Pb zircon dating

Zircons were separated from the coarse grained and less deformed metagabbroic rocks (see Fig. 3) collected from Antas (ANT-), St. Lourenço (AF-) and Oriola (OR-) IOMZOS (horneblende gabbros: ANT-1-7 and AF-3; gabbronorite; OR-1-2), using conventional heavy liquid and magnetic techniques, then hand-picked under binocular microscope. The metagabbros with the same transitional N/E-MORB geochemistry and the same mineralogical features of those observed in the IOMZOS metabasalts are cogenetic with the overall IOMZOS magmatic suite (Fonseca et al., 1999; Pedro, 2004; Araújo et al., 2005; Pedro et al., 2005; 2006).

Despite the large amount (several kilograms from each outcrop) of processed rocks, the metagabbros yielded only a few utilizable zircon crystals. These zircon grains were mounted in an epoxy resin disc, polished and coated with a gold film. Zircons were studied under transmitted and reflected light as well as cathodoluminescence (CL; Fig. 10) to reveal their external and internal structures.

U-Pb isotopic analyses were performed using the Sensitive High-Resolution Ion Microprobe (SHRIMP-II) at the Beijing SHRIMP Center of the Chinese Academy of Geological Sciences (Beijing) through a SHRIMP Remote Control Work Station located at the Geochronological Research Center of the University of São Paulo (Brazil). Analytical procedures for zircon were similar to those described by

Compston et al. (1992), Williams (1998) and Song et al. (2002). The U-Pb isotope data were collected after five scans; a reference zircon TEM (417 Ma; Black et al., 2003) was analysed after every four spots. Data uncertainties in Table 2 are quoted at 1σ level. U-Pb isotopic data were evaluated using the software package ISOPLOT/Ex (version 2.4) of Ludwig (2001).

Zircons are present both as subhedral multifaceted fragments, with typical sizes between 106-88 μm, and as prismatic fragmental crystals, with typical sizes between 177-106 μm. CL images (Fig. 10) of the analysed zircons do not detect any xenocrystic cores, but display a faint to marked oscillatory zoning, consistent with the magmatic origin of their host rocks. Six zircon grains (2 from each IOMZOS - Antas, Oriola and S. Lourenço - outcrops) were analysed. The SHRIMP U-Pb isotopic results are summarised in Table 2 and illustrated in a conventional concordia plot (Fig. 11).

The analysed zircons have U contents of 118-268 ppm and Th contents of 143-326 ppm with high Th/U ratios of 1.03-2.55, supporting their magmatic genesis. Zircon SHRIMP analyses yielded an overall $^{206}Pb/^{238}U$ age range from 476±5 Ma to 497±6 Ma (1σ errors; Table 2) and $^{206}Pb/^{238}U$-$^{207}Pb/^{235}U$ Concordia ages of 477±8 Ma, 478±7 Ma and 495±9 Ma (2σ errors; Fig . 12) for Antas, Oriola and St. Lourenço IOMZOS, respectively.

The zircon $^{206}Pb/^{238}U$ ages suggest that the IOMZOS could represent diachronic (ca. 20 Ma; Late Cambrian - Early Ordovician) obduction of Rheic's oceanic lithosphere and pointing to a weighted mean age of 482.5±9.4 Ma (2σ, MSDW = 2.4, probability = 0.033; Fig. 12). However, if the age of 497.5±6.1 Ma (spot 5.1; Table 2) is excluded from the weighted mean average age, a best fit $^{206}Pb/^{238}U$ weighted mean age of 479.6±5.1 Ma (2σ, MSWD = 1.19, probability = 0.31) with lower MSDW and higher probability of concordance is achieved. Nevertheless, both weighted mean average ages (479.6±5.1 Ma; n = 5 and 482.5±9.4 Ma; n = 6) are statistically identical and indistinguishable within the analytical uncertainty and have the same geodynamic significance. Given the preliminary nature of this study and particularly the scarcity of age data, it is more advisable to adopt the age of ca. 480 Ma as a fair estimate for the IOMZOS protolith age.

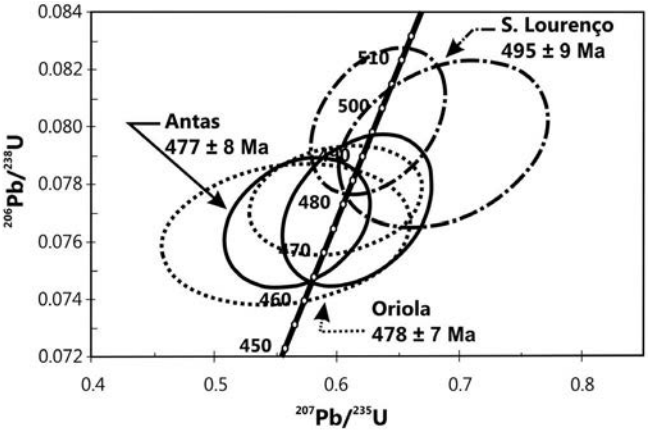

Fig. 11 - U-Pb concordia diagram of zircon SHRIMP data for the IOMZOS metagabbros (error ellipses are 2σ).

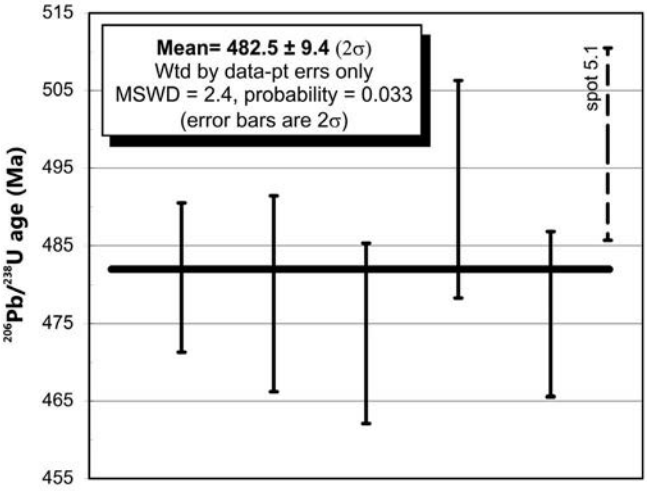

Fig. 12 - Weighted mean age diagram. Exclusion of the oldest 497.5±6.1 Ma, outlyer (spot 5.1), would give a statistically identical weighted mean average age of 479.6±5.1 Ma (2σ, MSWD = 1.19, probability = 0.31).

DISCUSSION

The geodynamic evolution of the SW Europe Variscides was recently summarised by Ribeiro et al. (2007). According to that work and the references therein, in SW Iberia, the BAOC and IOMZOS record ophiolite obduction, but only the internal oceanic klippen in OMZ (IOMZOS) should represent ophiolitic sequences originating from the Rheic Ocean. The Rheic Ocean (a wide ocean with passive margins which existed during Early Palaeozoic times) opened through a "rift-jump" from an intracratonic setting along the OMZ to intraoceanic rifting between the OMZ (IT) and the SPT. By contrast, BAOC is a back-arc obducted ophiolite derived from a minor ocean in a short-lived basin (Early-Middle Devonian) genetically related to the Rheic Ocean subduction under the SW border of OMZ (IT). This subduction process during Devonian times represents a mature stage of the Rheic Ocean (active margins) in SW Iberia.

Several lines of evidence correlate the IOMZOS with the Rheic Ocean in SW Iberia during the Early Ordovician: (1) the identification of a typical oceanic lithosphere sequence; (2) the whole-rock geochemical data indicative of ocean-floor basalts geochemistry (plume-proximal ridge system) that lack any orogenic and/or crustal contamination signature (despite the absence of isotopic data); and (3) the diachronic ages of 477±8 to 495±9 Ma that yield a weighted mean age of ca. 480 Ma. These evidences are in agreement with the geodynamic evolution model of the Rheic Ocean during the Early Paleozoic (Ribeiro et al., 2007; 2010) and, consequently, the above mentioned IOMZOS ages (477±8 to 495±9 Ma) have the same geodynamic significance. In this period, the Rheic Ocean in SW Iberia is believed to have been a well-developed ocean, with a typical oceanic lithosphere and a passive margins. This evolutionary stage is represented by the IOMZOS, which are fragments of the Rheic Ocean floor that were not consumed by subduction during the Late Paleozoic and were emplaced onto SW Iberia by obduction.

The OMZ Cambrian-Ordovician continental rifting migration and the IOMZOS are recorded respectively in the Neoproterozoic - Early Palaeozoic OMZ autochthonous rocks and in the allochthonous OMZ complexes. Two distinct evolutionary stages of the Rheic Ocean during the Early Ordovician can be observed from northeast (Sanchez-Garcia et al., 2003; Linnemann et al., 2008) to southwest

(Chichorro et al., 2008): (1) an intracontinental rifting stage, with crustal contamination in the mantle sources, is recorded as shallow plutonic and volcanic rocks accompanied by coeval sedimentary successions in the OMZ autochthonous rocks; and (2) early/full divergent margin stage, with tholeiitic ocean-ridge magmatism, is recorded by the IOMZOS lithospheric cross-section in the southern margin of the IA (peri-Gondwanan terranes).

Based on the presented data, despite the diachronic and scarce IOMZOS age data, only the IOMZOS should be viewed as remnants of the Rheic Ocean, and the IOMZOS age of ca. 480 Ma should represent the Rheic Ocean age for SW Iberia. However, more geochronological and isotopic studies are required to improve the knowledge on the IOMZOS protoliths geodynamic evolution.

ACKNOWLEDGEMENTS

The authors acknowledge an anonymous reviewer and the Editor R. Tribuzio for the careful and constructive comments which helped to improve the manuscript. We also acknowledge the collaboration with our colleagues A. Jesus and M. Gaspar for the zircons separations as well as R. Fonseca and C. Ribeiro for the text revision.

A special thank to our colleague J. Munhá who guided the idea of this paper and gave us all the scientific support.

This work was funded by FCT through CeGUL (Project POCA-PETROLOG POCTI/ISFL-5-263) and CGE.

REFERENCES

Araújo A., Fonseca P., Munhá J. Moita P., Pedro J. and Ribeiro A., 2005. The Moura Phyllonitic Complex: An Accretionary Complex related with obduction in the Southern Iberia Variscan Suture. Geodin. Acta, 18 (5): 375-388.

Black L.P., Kamo S.L., Allen C.M., Aleinkoff J.N., Davis D.W., Korsch R.J. and Foudoulis C., 2003. TEMORA 1: a new zircon standard for Phanerozoic U-Pb geochronology. Chem. Geol., 200: 155-170.

Chichorro M., Pereira M.F., Díaz-Azpiroz M., Williams I.S., Férnandez C., Pin C. and Silva J.B., 2008. Cambrian ensialic rift-related magmatism in the Ossa-Morena Zone (Évora - Aracena metamorphic belt, SW Iberian Massif): Sm-Nd isotopes and SHRIMP zircon U-Th-Pb geocronology. Tectonophysics, 461: 91-113.

Compston W., Williams I.S., Kirschvink J.L., Zhang Z. and Guogan M., 1992. Zircon U-Pb ages for the Early Cambrian timescale. J. Geol. Soc. London, 149: 171-184.

Dias R., Araújo A., Terrinha P. and Kullberg J.C., 2006. Geologia de Portugal no Contexto da Ibéria. Évora Univ., Évora (Portugal), 418 pp.

Eguiluz L., Gil Ibarguchi J.I., Abalos B. and Apraiz A., 2000. Superposed Hercynian and Cadomian orogenic cycles in the Ossa-Morena zone and related areas of the Iberian Massif. Geol. Soc. Am. Bull., 112: 1398-1413.

Etxebarria M., Chalot-Prat F., Apraiz A. and Eguiluz L., 2006. Birth of a volcanic passive margin in Cambrian time: Rift paleogeography of the Ossa-Morena Zone, SW Spain. Precamb. Res., 147: 366-386.

Expósito I., Simancas J.F., González Lodeiro F., Azor A. and Martínez Poyatos D.J., 2002. Estructura de la mitad septentrional de la Zona de Ossa Morena: deformación en el bloque inferior de un cabalgamiento cortical de evolución compleja. Rev. Soc. Geol. España, 15: 3-14.

Expósito I., Simancas J., González Lodeiro F., Bea F., Montero P. and Salman K., 2003. Metamorphic and deformational imprint of Cambrian - Lower Ordovician rifting in the Ossa-Morena Zone (Iberian Massif, Spain). J. Struct. Geol., 25: 2077-2087.

Flower M., 1991. Magmatic process in oceanic ridge and intraplate settings. In: P.A. Floyd (Ed.), Oceanic basalts. Blackie and Son, London, p. 116-147.

Floyd P.A., 1991. Oceanic islands and seamounts. In: P.A. Floyd (Ed.), Oceanic basalts. Blackie and Son, London, p. 174-218.

Fonseca P., 1995. Estudo da Sutura Varisca no SW Ibérico nas regiões de Serpa-Beja-Torrão e Alvito-Viana do Alentejo. PhD Thesis, Lisboa Univ., Lisboa, 325 pp.

Fonseca P., Munhá J., Pedro J., Rosas F., Moita P., Araújo A. and Leal N., 1999. Variscan ophiolites and high-pressure metamorphism in Southern Iberia. Ofioliti, 24 (2): 259-268.

Giese U. and Bühn B. 1994. Early Paleozoic rifting and bimodal volcanism in the Ossa-Morena Zone of south-west Spain. Geol. Runds., 83: 143-160.

Gill J., 1981. Orogenic andesites and plate tectonics. Springer, Berlin, 390 pp.

Green T.H., 1995. Significance of Nb/Ta as an indicator of geochemical process in the crust-mantle system. Chem. Geol., 120: 347-359.

Hannigan R., Basu A and Teichmann F., 2001. Mantle reservoir geochemistry from statistical analysis of ICP-MS trace element data of equatorial mid-Atlantic MORB glasses. Chem. Geol., 175: 397-428.

Jesus A., Munhá J., Mateus A., Tassinari C. and Nutman A., 2007. The Beja Layered Gabbroic Sequence (Ossa-Morena Zone, Southern Portugal): geochronology and geodynamic implications. Geodin. Acta, 20 (3): 139-157.

Juteau T. and Maury R., 1999. The oceanic crust, from accretion to mantle recycling. Springer-Praxis, Berlin, 390 pp.

Le Bas M.J., Le Maitre R.W., Streckeisen A. and Zanettin B., 1986. A chemical classification of volcanic rocks on the total alkali silica diagram. J. Petrol., 27 (3): 745-750.

Le Maitre R.W., Bateman P., Dudek A., Keller J., Lameyre J., Le Bas M.J., Sabine P.A., Schmidt R., Sorensen H., Streckeisen A., Woolley A.R. and Zanettin B., 1989. A classification of igneous rocks and glossary of terms. Blackwell Publ., Oxford, 193 pp.

Linnemann U., Pereira M.F., Jeffries T., Drost K. and Gerdes A., 2008. Cadomian orogeny and the opening of the Rheic Ocean: New insights in the diachrony of geotectonic processes constrained by LA-ICP-MS U-Pb zircon dating (Ossa-Morena and Saxo-Thuringian Zones, Iberian and Bohemian Massifs). Tectonophysics, 461: 21-43.

Ludwig K.R., 2001. Users manual for Isoplot/Ex (rev. 2.49): a geochronological toolkit for Microsoft Excel. Berkeley Geochron. Center, Spec. Publ., 1a, 55pp.

Mata J. and Munhá J., 1990. Magmatogénese de metavulcanitos câmbricos do nordeste alentejano: os estádios iniciais de "rifting" continental. Comun. Serv. Geol. Portugal, 76: 61-89.

Matte Ph., 1986. Tectonics and plate tectonics models for the Variscan Belt in Europe. Tectonophysics, 126: 329-374.

Middlemost E.A.K., 1975. The basalt clan. Earth Sci. Rev., 11: 7-51.

Middlemost E.A.K., 1989. Iron oxidation ratios, norms and the classification of volcanic rocks. Chem. Geol., 77: 19-26.

Miyashiro A., 1974. Volcanic rock series in island arcs and active continental margins. Am. J. Sci., 274: 321-355.

Miyashiro A., 1994. Volcanic rock series in island arcs and active continental margins. Am. J. Sci., 274: 321-355.

Moita P., Munhá J., Fonseca P., Pedro J., Tassinari C., Araújo A. and Palácios T., 2005. Phase equilibria and geochronology of Ossa-Morena eclogites. ActasIV Semana de Geoquímica - 8th Congr. Geoquím. Países Língua Portuguesa, 2: 471-474.

Moita P., Santos J. F. and Pereira M.F., 2009. Layered granitoids: Interaction between continental crust recycling processes and mantle-derived magmatism. Examples from the Évora Massif (Ossa-Morena Zone, southwest Iberia, Portugal). Lithos, doi: 10.1016/j.lithos.2009.02.00.

Mullane M., 1998. The geochemistry of the South Portuguese Zone, Spain and Portugal. PhD Thesis, Southampton Univ., Southampton, 467 pp.

Munhá J., Oliveira J.T., Ribeiro A., Oliveira V., Quesada C. and Kerrich R., 1986. Beja-Acebuches ophiolite characterization and geodynamic significance. Maleo, 2 (13): 31.

Niu Y., Bideau D., Hékinian R. and Batiza R., 2001. Mantle compositional control on the extent of mantle melting, crust production, gravity anomaly, ridge morphology, and ridge segmentation: a case study at the Mid-Atlantic Ridge 33-35º N. Earth Planet. Sci. Lett., 186: 383-399. Supplementary data - http://www.sciencedirect.com/science/MiamiMultiMediaURL//B6V61-42R0T1R-5/B6V6142R0T1R5/5801/html

Pearce J., 1982. Trace element characteristics of lavas from destructive plate boundaries. In: R. Thorpe (Ed.), Andesites, Wiley, Chichester, p. 525-548.

Pearce J., 1983. Role of sub-continental lithosphere in magma genesis at active continental margins. In: C.J. Hawkesworth and M.J. Nurry (Eds.). Continental basalts and mantle xenoliths, Shiva Publishing, Nantwich, p. 230-249.

Pearce J., 2008. Geochemical fingerprinting of oceanic basalts with applications to ophiolite classification and the search for Archean oceanic crust. Lithos, 100: 14-48. doi: 10.1016/j.lithos.2007.06.016

Pearce J. and Cann J., 1973. Tectonic settings of basic volcanic rocks determined using trace element analyses. Earth Planet. Sci. Lett., 19: 290-300.

Pearce J. and Peate D., 1995. Tectonic implications of the composition of volcanic arc magmas. Annu. Rev. Earth Planet. Sci., 23: 251-285.

Pedro J., 2004. Estudo geológico e geoquímico das sequências ofiolíticas internas da Zona de Ossa-Morena (Portugal). PhD Thesis, Évora Univ. Évora (Portugal), 225 pp.

Pedro J., Araújo A., Fonseca P. and Munhá J., 2005. Internal Ossa-Morena Zone ophiolitic sequences: geodynamic implications for the evolution of the SW branch of the Iberian Variscan Chain. Cad. Lab. Xeol. Laxe, 30: 235-258.

Pedro J., Araújo A., Fonseca P. and Munhá J., 2006. Ofiolitos e metamorfismo de alta pressão. In: R. Dias, A. Araújo P. Terrinha P. and J. Kullberg (Eds.), Geologia de Portugal no contexto da Ibéria. Évora Univ., Évora (Portugal), p. 195-206.

Quesada C., 1991. Geological constraints on the Paleozoic tectonic evolution of tectonostratigraphic terranes in the Iberian Massif. Tectonophysics, 185: 225-245.

Quesada C., 1992. Evolución tectónica del Maciço Ibérico. In: J.C. Gutierrez-Marco, J. Saavedra and I. Rábano (Eds.), Paleozoico Inferior de Ibero-América. Univ Extremadura, p.173-190.

Quesada C., 1997. Evolución geodinamica de la Zona de Ossa-Morena durante el ciclo Cadomiense. In: A. Araújo and M.F.C. Pereira (Eds.), Estudos sobre a geologia da Zona de Ossa-Morena (Maciço Ibérico). Évora Univ., Évora (Portugal), p. 205-230.

Quesada C., 2006. The Ossa-Morena Zone of the Iberian Massif: a tectonostratigraphic approach to its evolution. Ges. Geowiss., 157: 585-595.

Quesada C., Fonseca P., Munhá J., Oliveira J. and Ribeiro A., 1994. The Beja-Acebuches Ophiolite (Southern Iberia Variscan Foldbelt): geological characterization and geodynamic significance. Bol. Geol. Minero España, 105 (1): 3-49.

Ribeiro A., Munhá J., Dias R., Mateus A., Pereira E., Ribeiro L., Fonseca P., Araújo A., Oliveira T., Romão J., Chaminé H., Coke C. and Pedro J., 2007. Geodynamic evolution of the SW Europe Variscides. Tectonics, 26, TC6009 (doi:10.1029/2006 TC002058, 170 2007).

Ribeiro A., Munhá J., Fonseca P., Araújo A., Pedro J., Mateus A., Tassinari C,. Machado G. and Jesus A., 2010. Variscan Ophiolite Belt in the Ossa-Morena Zone (Southwest Iberia): Geological characterization and geodynamic significance. Gondw. Res., 17: 408-421.

Ribeiro A., Quesada C. and Dallmeyer R.D., 1990. Geodynamic evolution of the Iberian Massif. In: R.D. Dallmeyer and E. Martinez Garcia (Eds.), Pre-Mesozoic geology of Iberia, Springer-Verlag, p. 398-409.

Rollinson H., 1993. Using geochemical data: evaluation, presentation, interpretation. Longman Group, London, 352 pp.

Romeo I., Lunar R., Capote R., Quesada C., Piña R., Dunning G.R. and Ortega L., 2006. U/Pb age constraints on Variscan magmatism and NiCuPGE metallogeny in the Ossa-Morena Zone (SW Ibéria). J. Geol. Soc. London, 163: 1-9.

Roux P., Roex A., Schiling J., Shimizu N., Perkins W. and Pearce N., 2002. Mantle heterogeneity beneath the southern Mid-Atlantic Ridge: trace elements evidence for contamination of ambient asthenospheric mantle. Earth Planet. Sci. Lett., 203: 479-498.

Sanchez-Garcia T., Bellido F. and Quesada C., 2003. Geodynamic setting and geochemical signatures of Cambrian-Ordovician rift-related igneous rocks (Ossa-Morena Zone, SW Iberia). Tectonophysics, 365: 233-255.

Simancas J.F., Carbonell R., González Lodeiro F., Pérez Estaún A., Juhlin C., Ayarza P., Kashubin A., Azor A., Martínez Poyatos D., Almodóvar G.R., Pascual E., Sáez R. and Expósito I., 2003. The crustal structure of the transpressional Variscan Orogen of SW Iberia: The IBERSEIS Deep Seismic Reflection Profile. Tectonics, 22: 1062 (doi: 10. 1029/2002TC001479).

Simancas J.F., Martínez Poyatos D.J., Expósito I., Azor A. and González Lodeiro F., 2001. The structure of a major suture zone in the SW Iberian Massif: the Ossa Morena / Central Iberian contact. Tectonophysics, 332: 295-308.

Song B., Zhang Y.H., Wan Y.S. and Jian P., 2002. Mount making and procedure of the SHRIMP dating. Geol. Rev., 48: 26-30.

Sun S., 1980. Lead isotopic study of young volcanic rocks from mid-ocean ridges, ocean islands and island arcs. Phil. Trans. R. Soc., A297: 409-445.

Sun S. and McDonough W., 1989. Chemical and isotopic systematics of oceanic basalt: implications for mantle composition and processes In: A. Saunders and J. Norry (Eds.), Magmatism in oceanic basins. Geol. Soc. London Spec. Publ., 42: 313-345.

Sun S. and Nesbitt R., 1977. Chemical heterogeneity of the Archean mantle, composition of the bulk earth and mantle evolution. Earth Planet. Sci. Lett., 35: 139-155.

Sun S. and Nesbitt R., 1978. Geochemical regularities and genetic significance of ophiolitic basalts. Geology, 28: 689-693.

Sun S., Nesbitt R. and Sharaskin A., 1979. Geochemical characteristics of mid-ocean ridge basalts. Earth Planet. Sci. Lett., 44: 119-138.

Vera J.A., 2004. Geologia de España. Serv. Geol. España/Inst. Geol. Miner. España (SGE/IGME), Madrid, 890 pp.

Williams I.S., 1998. U-Th-Pb geochronology by ion microprobe. In: M.A. McKibben, W.C. Shanks and W.I. Ridley (Eds.), Applications of microanalytical techniques to understanding mineralizing processes. Rev. Econ. Geol., 7: 1-35.

Wilson M., 1989. Igneous petrogenesis: A global tectonic approach. Chapman & Hall, London, 466 pp.

Wood D.A., 1980. The application of a Th-Hf-Ta diagram to problems of tectonomagmatic classification and to establishing the nature of crustal contamination of basaltic lavas of the British Tertiary volcanic province. Earth Planet. Sci. Lett., 50: 11-30.

Received, May 28, 2010
Accepted, December 1, 2010